PCCP

Accepted Manuscript

ROYAL SOCIETY OF CHEMISTRY

www.rsc.org/pccp

Reactive Simulations-based Model for the Chemistry behind Condensed Phase Ignition in RDX crystals from Hot Spots

Kaushik L Joshi, Santanu Chaudhuri*

Illinois Applied Research Institute

University of Illinois at Urbana-Champaign, Champaign IL 61820

Abstract

Chemical events that lead to thermal initiation and spontaneous ignition of high-pressure phase of RDX are presented using reactive molecular dynamics simulations. In order to initiate the chemistry behind thermal ignition, approximately 5% of RDX crystal is subjected to a constant temperature thermal pulse of various time durations to create hot spots. After application of the thermal pulse, the ensuing chemical evolution of the system is monitored using reactive molecular dynamics under adiabatic conditions. Thermal pulse above certain time durations leads to the spontaneous ignition of RDX after an incubation period. For cases where the ignition is observed, the incubation period is dominated by intermolecular and intramolecular hydrogen transfer reactions. Contrary to the widely accepted unimolecular models of initiation chemistry, N-N bond dissociations that produce NO_2 species are suppressed in the condensed phase. The gradual temperature and pressure increase in the incubation period is accompanied by the accumulation of short-lived heavier polyradicals. The polyradicals have the triazine rings from the RDX molecules intact. At certain temperature and pressure, the polyradicals undergo the ring-opening reactions which fuel a series of rapid exothermic chemical reactions leading to the thermal runaway regime with stable gas-products such as N_2, H_2O and CO_2. The evolution of the RDX crystal through the thermal initiation, incubation and thermal runaway phases observed in the reactive simulations contains a rich description of condensed-phase chemistry of nitramines under high-temperature/pressure conditions.

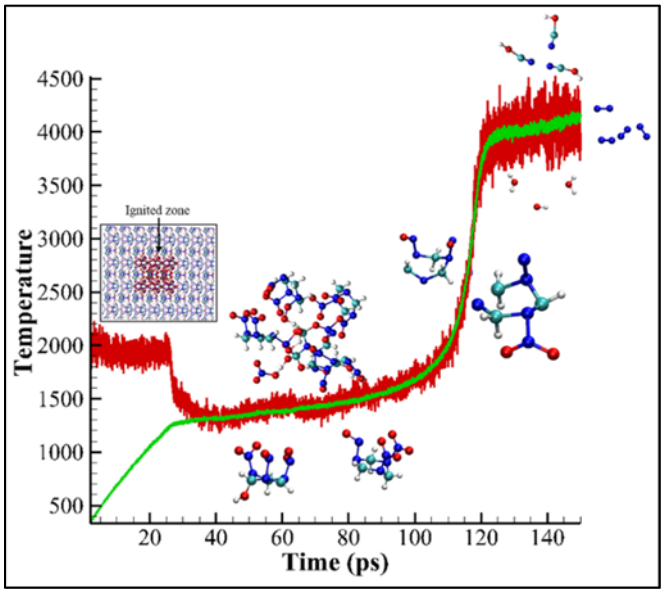

Introduction

Chemical events that lead to the ignition of solid propellants and energetic material have fascinated many disciplines of science and engineering for a long time. Classical theories of the ignition of solids started to be formalized by researchers such as Zeldovich in 1940s[1]. Highly reactive nitramine-based materials such as Hexahydro-1,3,5-trinitro-1,3,5-triazine (RDX) are model energetic molecules and the chemistry of their ignition characteristics is important for many technological applications. The chemical steps that lead to the ignition in reactive solids are complex and hard to follow using the experimental probes. The ignition of energetic materials (EM) can be achieved through different initiating conditions such as thermal, laser or shock wave initiations. In all cases, the high temperatures regions inside the solids called hot spots are used to describe the prerequisite conditions for ignition. It is assumed that under right temperature and size, the spontaneous ignition can be achieved for an EM. Depending on the chemistry and the external conditions, the rapid burn (deflagration) can be followed by the detonation events. Thus, the safety and performance of the formulations of EM depends on the ability to understand the chemical events from initiations through ignition stages. Currently, there is no direct measurement of the critical hot spot temperature and the size needed for the ignition of solid RDX. It is widely accepted that the self-sustaining ignition front from a hot spot is net exothermic and the complex chemistry is buried in thousands of reactive events inside the solid around the hot spot. It is also expected that some of the reaction mechanisms valid for the gas-phase reactions in RDX are going to be modified in RDX under high temperature and compression. Most of the previous studies that have focused on the gas-phase thermal decomposition of RDX widely believe that the unimolecular decomposition mode is more dominant in gas-phase and occurs mainly through the following 3 different mechanisms, (1) Homolytic cleavage of an N-N bond [2-3] to NO_2, (2) Concerted decomposition to form three methylene nitramines (CH2=N-NO2)[3-4], (3) HONO elimination to form three successive HONO and 1,3,5-triazine[5-6] These primary decomposition mechanisms are followed by the various secondary reactions that are sensitive to the temperature and pressure. Significant efforts have been made in the past to combine these primary reactions with the secondary reaction channels to form the complete mechanism for RDX combustion [7-8]. More detailed mechanistic information about the thermal decomposition and combustion of the gas-phase RDX can be found in a recent article by Kuo and Acharya[9]

Little mechanistic information is available on the exact order of the decomposition events in the condensed-phase RDX under high temperature and pressure conditions that lead to ignition and propagation of self-sustaining reactions in the solid. Some experimental studies have investigated the decomposition chemistry at the surface-vapor interface [10-11]. However, the observed kinetics were influenced by the gas-phase mechanisms and the sublimation at the solid-vapor interface. In literature, some experimental and theoretical studies suggest that the mechanism of condensed-phase decomposition can be significantly different from the gas-phase. For example, Wang et al. studied the thermal decomposition in dilute solution under high pressure and found that the homolytic N-N cleavage (primary channel for producing NO_2) is fully suppressed in solvated RDX [12]. Recently, DFT-based MD simulations were performed to study the decomposition of molten RDX at high temperatures and pressures[13]. The author found that the number of N-N bond breaking events decreases with increase in the density while the number of C-H bond breaking events remain the same for various densities. However due to the higher computational cost, the simulations were done on the small system containing only 8 molecules. Recently, Brennan et al.[14] simulated the shock compression of RDX crystal using Dissipative Particle Dynamics (DPD). A reduced chemical model consisting of one unimolecular and three bimolecular reactions was proposed as the essential chemistry for the initiation and propagation reactions.

Other atomistic scale methods such as reactive molecular dynamics (RMD) have the potential to provide a direct description of various chemical mechanisms that eventually lead to ignition and detonation of RDX. ReaxFF is the reactive force field [15] that can model bond formation and bond breaking on the fly during MD simulations. The detailed information about ReaxFF can be found in Chenworth et al.[16]. Strachan et al [17]studied the thermal decomposition of RDX at various temperatures and densities using ReaxFF. However, those simulations were done on a very small system containing only 8 molecules and so could not provide detailed reaction channels of the RDX ignition chemistry. ReaxFF has also been used to study the thermal decomposition of other EM such as nitromethane[18], ammonium nitrate[19], HMX[20-21], TNT[22], PETN[23]. Besides thermal decomposition, ReaxFF has also been employed to study the hot spot formation and detonation [24-25] and to investigate the role of defects in energetic crystals[26]. In part, the RMD literature discussed above is concentrated mostly on the constant temperature canonical ensemble (NVT) which does not provide the opportunity to identify the adiabatic observation of

the steps needed for ignition from a hot spot. Other efforts comparable to RMD simulations include the study of HMX and TATB decomposition using tight-binding approaches (DFTB) at high temperatures. The authors compared the chemistry from DFTB simulations with the CHEETAH code predictions.[27-29] Analysis of the larger fragments such as the nitrogen containing polycyclic intermediates identified in such simulations under high compression is a complex challenge. Recently, efforts have been made to design the protocol for analyzing the complex chemistry that occurs during the thermal decomposition of hydrocarbons and dense materials[30-31]. However, none of the previous studies have provided the details of chemical mechanisms that lead to thermal runaway process in solid-phase RDX from a hot spot. In this work, we intend to develop a chemical model to provide valuable insight into this missing mechanistic description on how hot spots, created by thermal pulse, can ignite perfect RDX crystals under adiabatic conditions.

Simulating hot spots created by the excited electronic states is beyond the scope of this work due to the method and time-scale limitations. Instead, the hot spot is created by providing a thermal pulse to a small portion of the perfect crystal for different time durations. The small size of the hot spot in RMD simulations is expected to provide a lower limit on the size of the hot spot and the upper limit on critical temperature due to the inverse scaling relationship known between the hot spot size and the critical temperatures.[32] With this setup, the current work uses RMD simulations to investigate two important questions related to ignition of RDX: (a) How does the critical temperature at the hot spot in perfect RDX crystals determine the ignition and growth under adiabatic conditions? (b) How to provide a kinetic descriptions of reactive events which drives the growth? As such, these simulations are numerical experiments based on ReaxFF to ignite the high-density reactive phase of solid RDX from the hot spot of different temperatures to identify the chemistry behind self-sustained ignition that leads to a thermal runaway. Validation of the chemistry is essential for placing full confidence in these results or for improving the force field using better training sets. As a result, we demonstrate some preliminary results using DFT and higher level theory (MP2) to validate some key events seen in this RMD simulation trajectories.

Simulation Method

We have performed the simulations to capture the following three stages of a thermal ignition experiment: (1) an external stimulus supplies heat to a part of the solid to form a hot spot (*Thermal Pulse*), (2) On removal of the stimulus, an incubation period can be observed (*ignition*

delay) until the reactive chemistry leads to a critical point, (3) After reaching the criticality, a spontaneous ignition and possibly a deflagration state can be achieved (*thermal runaway*). The simulations were performed on the high-pressure γ-phase[33] with an experimental density of 2.26 gm/cm^3. The choice of γ-RDX over stable α-phase was prompted by experimental evidence[33] using Raman spectroscopy of shock-initiated RDX that the chemical decomposition propagates mainly through high-pressure γ-phase. The starting geometry of the unit cell of the γ-phase was obtained from density functional theory (DFT) calculations as implemented in the CASTEP program and van der Waals corrected DFT-D calculations at the PBE level.[34] The quantum unit cell was then energy minimized with ReaxFF to relax the atomic positions. The larger supercell containing 512 RDX molecules was created by expanding the unit cell to 4×4×4 matrix (50.24Å × 37.92 Å × 43.68 Å).

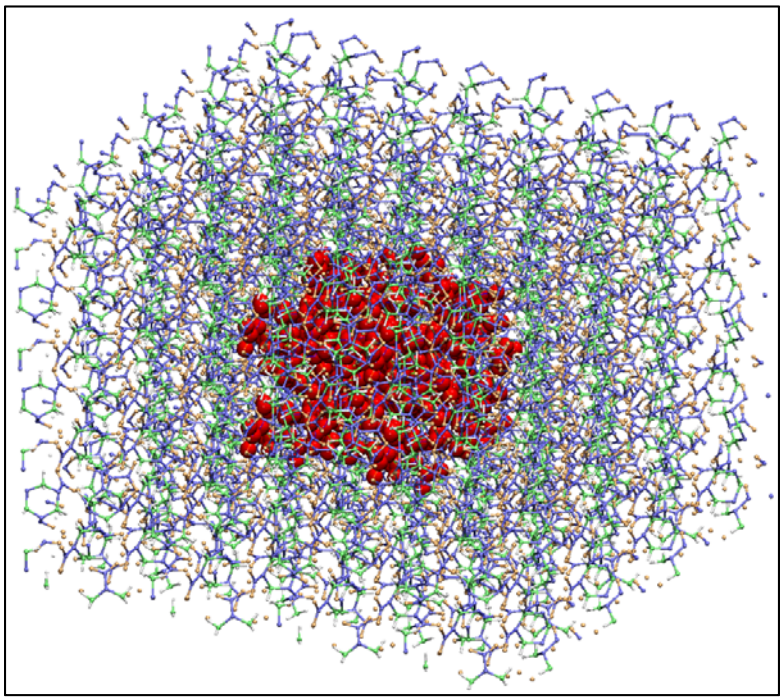

Figure 1: 3-D view of the periodic simulation cell containing the hot-spot at the center of the cell as shown by the red colored region. For the rest of the cell, color scheme is as follows: Nitrogen - Blue, Oxygen - Orange, Carbon - Green, Hydrogen - White

The supercell was initially equilibrated for 100,000 time steps at 300K with a time step of 0.01fs. During the equilibration step, we did not observe any change in the chemical composition of the system and all the RDX molecules were chemically intact. This equilibrated system was then used for all the remaining MD simulations. To mimic the hot spots, a collection of 24

molecules (≈ 6 % by volume) at the center of the simulation box (Figure 1) was subjected to a thermal pulse to attain a constant temperature for various time durations or pulse width. During the thermal pulse duration, the temperature of the atoms belonging to the hot spot was maintained at 1000K and 2000K using NVT ensemble while the rest of the system was integrated using the NVE ensemble. Duration of the thermal pulse was varied from 5ps to 40ps in our current study. The 1000 K hot spot did not attain criticality. Therefore, results from the 2000 K hot spots created using the thermal pulse are reported here. Due to the small time window available to MD simulations (nanoseconds), the thermal pulse applied to the small number of RDX molecules is a means to overdrive the chemistry and mimic the hot spots which can form during laser ignition or shock compression through various mechanisms. Once the thermal pulse duration is over, then the entire system was integrated using NVE ensemble. Due to the high density of γ phase and the fast chemistry of the energetic materials, we have used a conservative time step of 0.01 fs in all the simulations to ensure that faster local equilibrium can be achieved between the newly created species.

The reactive MD calculations were performed using ReaxFF implementation[35] that is available in LAMMPS[36] MD suite. The simulations were performed with the force field parameters published in Wood et al.[21] The original CHNO parameters were trained against an extensive training set that consisted of the different chemical reactions that are important for RDX combustion[17].The force field used in this work was obtained by integrating that original ReaxFF nitramine (C/H/N/O) training set with C/H/O combustion training set[16]. The resulting parameters are fully transferable with the combustion branch of ReaxFF and can provide an enhanced description of the C/H/O combustion chemistry applicable to energetic materials. It has been shown that ReaxFF-lg[37] formalism provides better description for London dispersion than the original ReaxFF. The supporting information contains comparison between ReaxFF and ReaxFF-lg for γ-RDX. Since the high pressure γ-phase at elevated temperatures was used in reactive simulations and providing the deeper atomistic chemistry is the main focus of this work, we have used the original formulation of ReaxFF that is capable of providing an enhanced description of the combustion chemistry.

Results

Effect of thermal pulse duration on RDX ignition

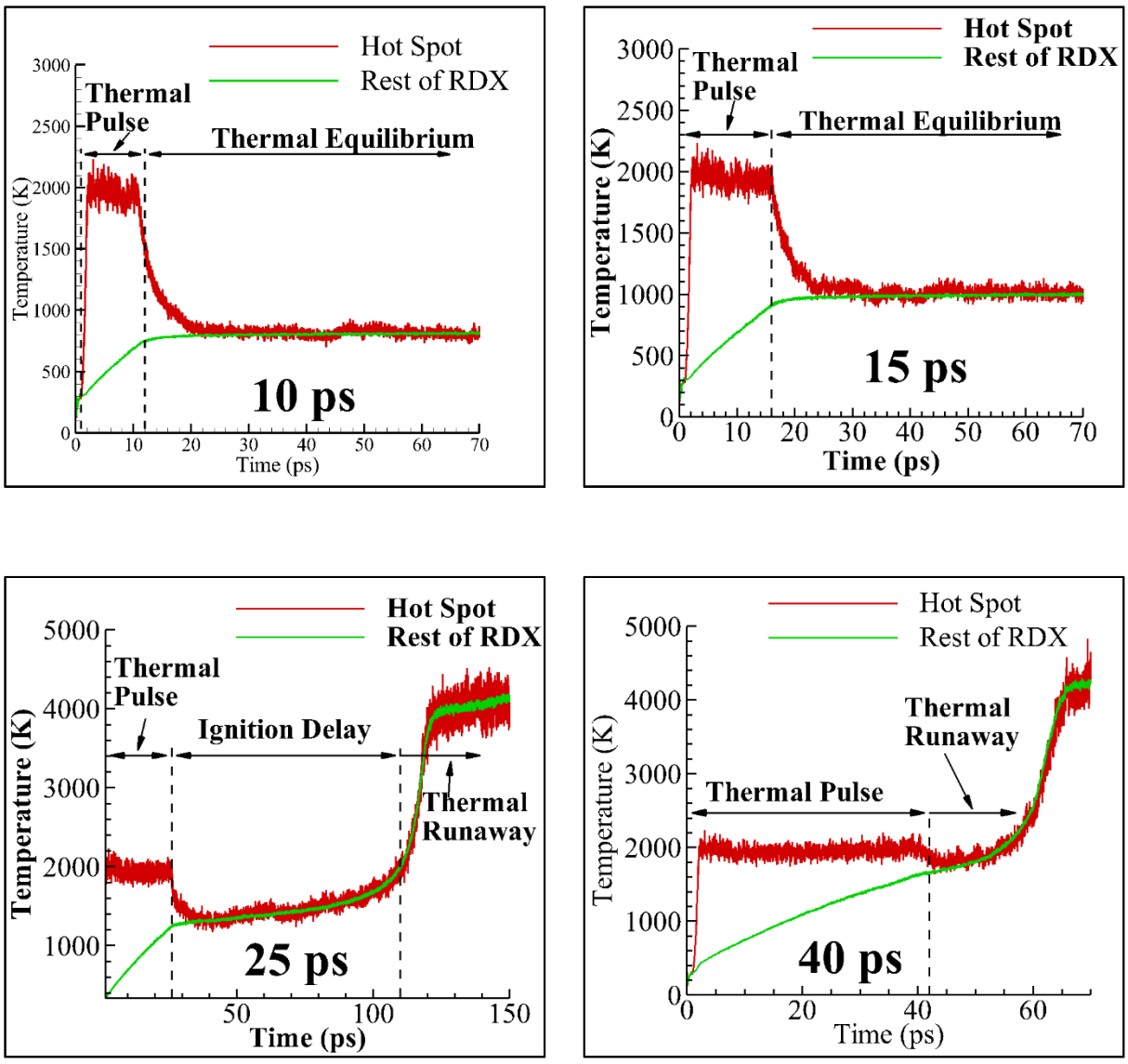

Figure 2: Effect of thermal pulse duration on the temperature profiles of externally ignited hot spot and non-ignited zones of RDX. The ignited hot spots are 5% of the total simulation domain and comes to equilibrium with rest of the RDX molecules fast. The effect of heat transfer from the hot spots is visible in the duration of the incubation period before thermal runaway is observed.

Figure 2 shows the effect of the duration of the thermal pulse on the temperature of the RDX crystal. It can be seen that due to the energy transfer from the hot spot at the center of the domain to the non-ignited zone (treated using NVE ensemble), the temperature of the non-ignited zone increases until the entire system reaches equilibrium at some intermediate temperature. For

the thermal pulse of duration less than 15ps, the entire system equilibrates to a temperature that is less than or equal to 1000K. In the simulated time, no gradual increase in temperature is observed in these 15ps thermal pulse simulations. Such a behavior in hot spots is associated with the initiation sites that do not lead to a local ignition of the solid in the simulated time. In the longest thermal pulse simulated, (40ps), we observe the direct jump from thermal pulse regime into the thermal runaway regime indicating that the external thermal pulse is over-driving the system towards deflagration (Figure 2). For intermediate ignition duration (25ps), the overall system first equilibrates to 1300K at the end of the thermal pulse. After that, the system temperature continues to rise slowly up to ≈1700K. This gradual rise is due to combined effect of initial energy transfer from ignited zone and exothermic chemical reactions. In the classical definition of ignition, a criticality point is defined where net exothermic reactions exceed the net endothermic reactions in a reaction zone. In the current simulation, no such classical point in time is detected. Beyond 1700K (100ps), the entire crystal reacts spontaneously resulting into sharp increase in temperature by 2000K in 15ps. This sudden change in the temperature profile clearly shows a transition to different kinetic regime which can sustain a spontaneous reaction front. Since three distinct regimes were found in 25ps thermal pulse, we have used that simulation for the subsequent chemical mechanism analysis.

Figure 3a shows the potential energy and the kinetic energy variation during the three different regimes of the thermal decomposition in condensed phase RDX. It can be seen that the thermal pulse ignites the system to a higher energy state to facilitate the hot spot formation. During the ignition delay phase, the potential energy is slowly converted into the kinetic energy indicating that the overall system energy is conserved. In the thermal runaway regime, the rapid rise in kinetic energy is accompanied by a sharp decline in potential energy until 125 ps. Beyond 125 ps, the drift in total energy of the system is more than 1% and it continues to drift for the remaining 25ps (Figure 3a). The energy conservation depends upon many factors such as nature of potential energy surface, simulation step size etc. Since the chemistry of the thermal decomposition is very fast, we have already employed a very conservative time step of 0.01fs. However, the poor energy conservation at very high temperatures like 4300K indicates that even lower time step may be needed to satisfy the adiabatic conditions. In addition, since the force field parameters are not trained for all the discontinuities in the potential energy surfaces, such discontinuities may also violate the overall energy conservation. Until 125 ps, the drift in the total energy is less than 1%

which corresponds to less than 1 kcal/mol of energy per atom. As a result, the poor energy conservation beyond 125ps does not affect the overall chemistry presented in the article because most of the chemistry occurs before 125ps. Figure 3b shows that the sharp rise in temperature is accompanied by the corresponding sharp rise in pressure. The fully reacted state is reached at around 35 GPa pressure. The pressure is probably over-estimated in this simulation as addition of van der Waals correction to the force field may be required for improved description of the P-T states.

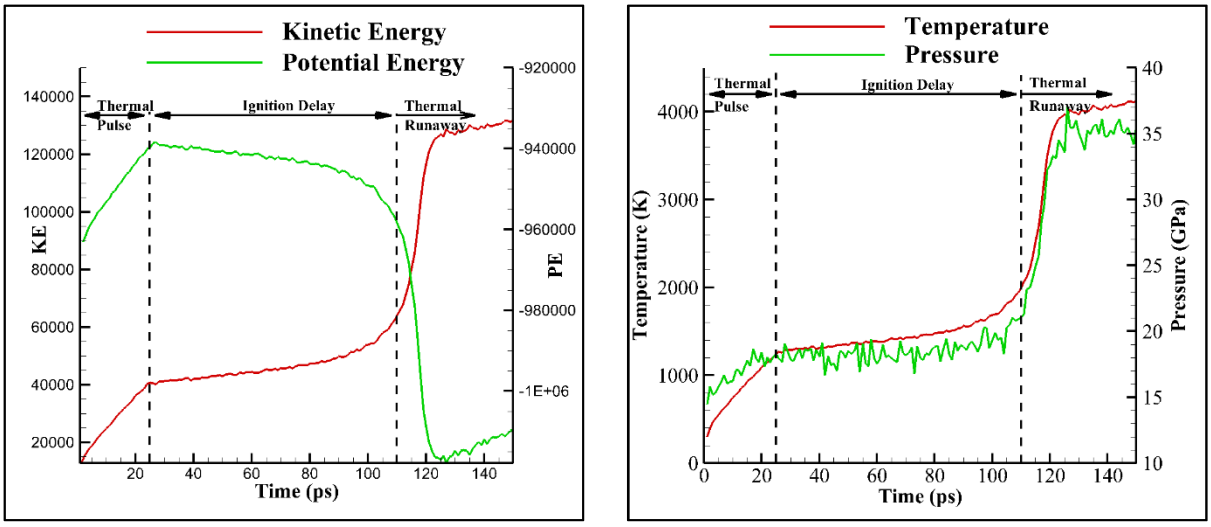

(a) (b)

Figure 3: Energy and pressure profiles obtained from reactive MD simulations, for the 25 ps thermal pulse case. The maximum pressure reached is 35 GPa, which is close to RDX Chapman-Jouget pressure of RDX.

The challenging task of ReaxFF simulations is extracting the chemical mechanisms from the immensely complex reactive MD trajectories. For example, in our calculation, nearly 150,000 reactive events are recorded during 150ps simulation. We have analyzed the trajectories without making any assumptions on the mechanisms. Using the software tools that were developed in-house, we have extracted all the chemical reactions that occurred during the RMD simulations. The fine grained chemistry for the initiation, ignition and growth of hot spot is presented next.

Triazine ring opening and formation of polyradicals

Figure 4a shows the rate of consumption of RDX molecules and RDX rings as a function of time. Bond order (BO) cut-off of 0.3 was used for identifying RDX molecules and rings for maintaining consistency with ReaxFF force field. The choice of the BO cut-off is based on the previous ReaxFF research studies on different types of systems. This choice of BO cut-off may alter molecule composition of some intermediate species and can be investigated further for finer resolution of the chemical species. It can be seen that all the RDX molecules react in less than 120ps and the observed consumption rate is approximately linear. During the thermal pulse (first 25ps), approximately 100 molecules were initiated which indicates that the remaining 80% of the RDX molecules remained chemically intact during the thermal stimuli. Although the RDX molecules steadily disappear with time, it can create a false impression of a faster decomposition kinetics. Instead, the concentration of the triazine rings can be used as an indicator of the energy content of the remaining reactants. Figure 4a also shows the rate of depletion of RDX rings (6-membered C-N heterocyclic ring) with time. In this analysis, a ring is counted only if all three 3 C-N bonds exist. The ring opening rate varies significantly with time compared to the analysis based on full RDX molecule. The initial ring opening rate up to 80ps is very slow as only 61 rings are broken during the ignition and the incubation period. During the same period, nearly 74% of the RDX molecules are initiated. A simplistic extrapolation of the same kinetics will mean that slight over 10% RDX in a less than $50nm^3$ domain is truly initiated at this incubation stage. The ring-opening rate gains considerable momentum for the next 30ps. During this duration (80ps to 110ps), 198 rings are broken at the approximate rate of 6 rings per picosecond, a sign of an ignition like kinetic behavior. The ring opening in this stage accelerates due to the creation of reactants needed to fuel the exothermic chemistry. After 110ps, we observe another sharp decline in the population of RDX rings at the rate of 25 rings per picosecond. This sudden burst of energy due to the ring openings causes the system temperature to rise sharply by 2000K in the next 15 picoseconds resulting in the thermal runaway. Figure 4a clearly shows that the triazine rings survive through different stages of reactions indicating that the disappearance of RDX molecules cannot be used as the only factor in determining the rate of reaction.

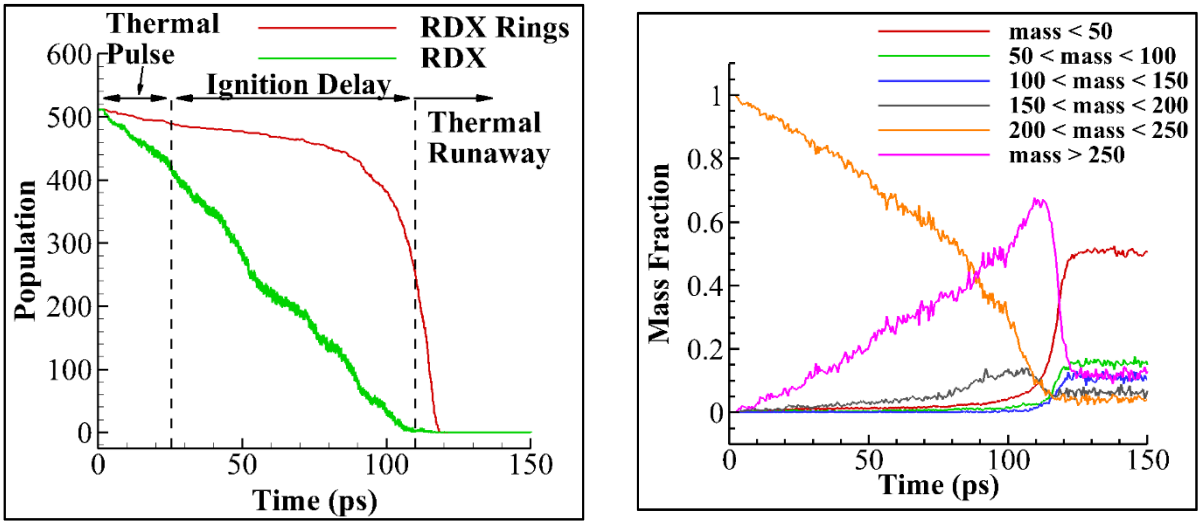

(a) (b)

Figure 4: Time evolution of RDX rings and mass fraction during ignition to thermal runaway transition

We used the mass fractions as our first filter for separating out the species because looking for specific gas-phase or a molecular radical species with known stoichiometry in these trajectories is prone to assumptions on mechanisms. Figure 4b shows the distribution and variation of mass fractions as a function of time. For the mass fraction analysis, the system was divided into 7 bins that are separated by 50amu and the corresponding mass fraction is calculated for each bin. The simulation shows that up to 120ps, most of the system is composed of heavier fragments (mass fraction > 200amu). In addition, the observed trend also indicates that with the decrease in RDX mass fraction (molecular weight of RDX is 222amu), the mass fraction of the molecular fragments that are heavier than RDX increases steadily before ring opening reactions happen. Figure 5 shows some of the heavier polyradicals that were observed in the reactive MD simulation. Strachan et al.[17] have reported the existance of large carbon clusters during the thermal decompsition of RDX at high densities. Although our simulations indicate the existance of heavy fragemtns, our molecular analysis and ring analysis clearly shows that such heavy fragements are primarily made of loosely coupled triazine rings instead of carbon clusters during the simulated time. It should be noted that due to the fast chemistry and high density, these heavier polyradicals have a very short life time (less than 10ps on most occasions) and hence they are constantly changing their chemical composition. However, the continued presense of heavier fragments (Figure 4b) clearly indicates that upon activation, the RDX molecules form short-lived, loosely coupled heavier polyradicals

instead of undergoing spontaneous decomposition into the smaller fragments. This deviation from the unimolecular decomposition based pathway is not surprising at the high-temperature/high-pressure conditions where the probability of bimolecular reactions is much higher. The mechanistic implications of the chemistry in such a high-density reactive ensemble are described next.

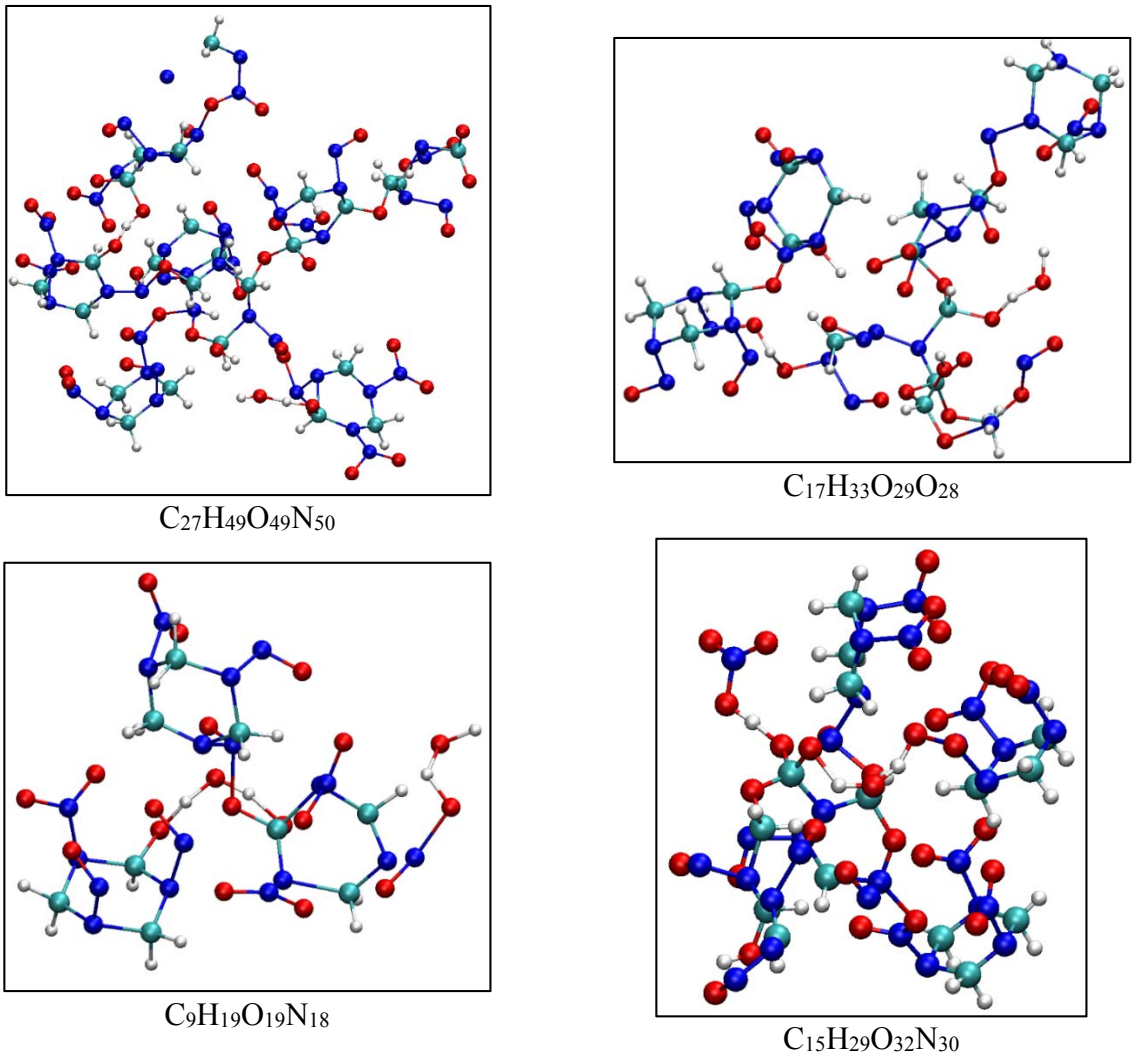

Figure 5: Snapshots of heavier fragments observed during reactive MD simulations, Nitrogen- Blue, Oxygen- Red, Carbon- Green, Hydrogen- White

Initiation mechanisms in γ-RDX

The mass fractions of molecular fragments and their subsequent interconversion between the mass-fraction bins allows one to interrogate the pathways for initiation stages. Figure 6 shows the dominant initiation pathways for the reactions that contain RDX monomer or dimer as

reactants. As seen in many dense and hot reactive mixtures, the most mobile species is H atom, which can exchange between the molecules many times causing the branching of reaction channels. Therefore, it is not surprising that intermolecular and intramolecular H transfer reactions dominate the initiation chemistry. Figure 6 shows that intermolecular H transfer via RDX dimer is the most dominant initiation mechanism. Nearly 12.5% of the neutral RDX is initiated by this bimolecular mechanism. The intermolecular H transfer can occur directly from CH_2 group or can be preceded by intramolecular H transfer to the oxygen of NO_2 group before dimerization (Figure 6). The unimolecular homolytic cleavage of N-N bond (leading to formation of NO_2) which is considered as the most dominant initiation pathway for the gas-phase RDX was observed only a few times (7 events) in our reactive MD simulation. This suppression of N-N bond cleavage in the high density phase of RDX qualitatively agrees with the recent DFT based-MD calculations[13].

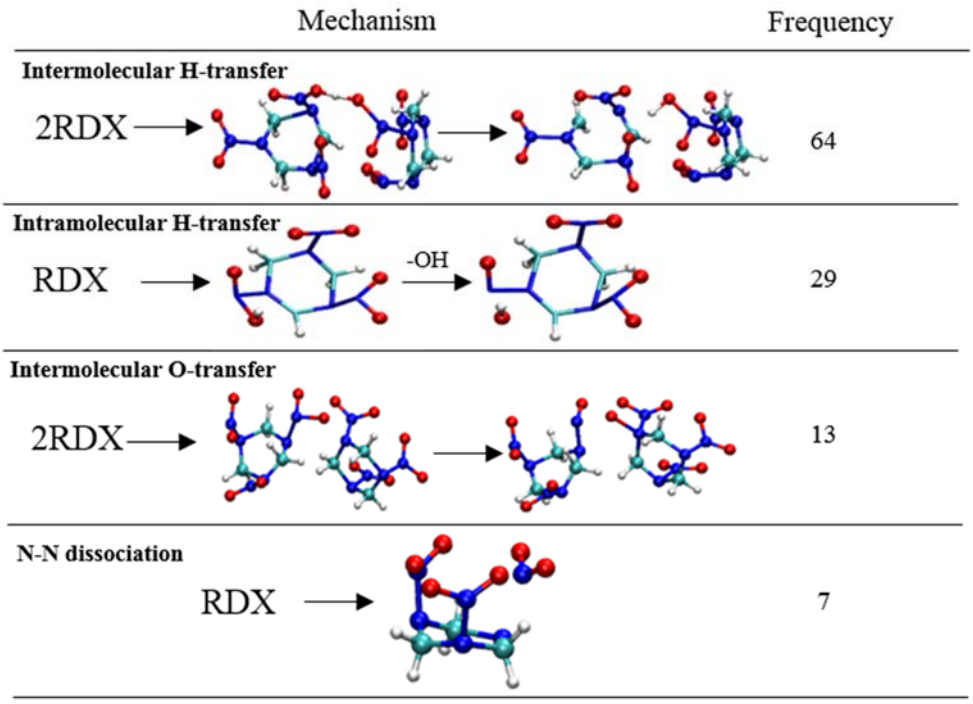

Figure 6: Condensed phase RDX initiation mechanisms: Primary steps and frequency of the events is indicated, Nitrogen- Blue, Oxygen- Red, Carbon- Green, Hydrogen- White

Figure 6 is still a simplification of many other events observed that lead to chemical transformation of RDX. For example, more than 1600 events corresponding to the isomerization of RDX molecule have been found. However, many of these isomers are short lived and eventually fall back to the original structure. In addition, we observed 93 events of RDX dimerization and

more than 70 events in which existing dimer breaks to form a new dimer with a different neighboring RDX molecule ($C_6H_{12}N_{12}O_{12} + C_3H_6O_6N_6 \longrightarrow C_3H_6O_6N_6 + C_6H_{12}O_{12}N_{12}$). After the bimolecular H transfer initiation mechanism, the 2nd most observed initiation mechanism involves a single RDX molecule. In this mechanism, the hydrogen from CH_2 group is first transferred to the NO_2 group of the same RDX molecule (intramolecular H transfer) which is then followed by the OH elimination forming $C_3H_5O_5N_6$ radical. This pathway of intramolecular H-transfer is known through DFT calculations. In addition to these hydrogen transfer reactions, we also observed some instances of initiation by oxygen transfer. Oxygen rich $C_3H_5O_7N_6$ radical formed by the intermolecular O-transfer reaction decomposes further either forming O_2 or extracts the hydrogen from the surrounding molecules to form OH.

Very little information is available in the literature about the activation energies of these different initiation mechanisms of RDX in condensed phase. In addition, the force field parameters that are used in these simulations were tested for important decomposition mechanisms only in gas phase RDX[17]. In order to obtain an estimate of the activation energies of these observed initiation mechanisms in condense phase γ-RDX, we performed the energy scans using ReaxFF on the following three initiation pathways, 1. N-N bond cleavage to form NO_2, 2. Intermolecular H transfer, 3. Intramolecular H transfer (Figure 7). The γ-phase unit cell configuration obtained from the DFT calculations was used for these energy scans. In each scan, the MD-based energy minimization was performed on each intermediate configuration[36]. During each energy minimization calculation, the atoms belonging to the reactant and the product state were allowed to relax, while the remaining atoms were frozen. Table 1 shows the estimated activation energies from ReaxFF for each of the three paths. It can be seen that the activation energy is higher in condensed phase than in gas phase for the NO_2 fomration[17]. This trend agrees with the DFT calculations that predicted the activation energy in excess of 60.0 kcal/mol on the same unit cell for NO_2 formation (See supporting information). Although, the intermolecular H transfer and NO_2 formation mechanisms have comparable activation energies, the heat of reaction for the intermolecular H transfer is significantly lower than the NO_2 formation. This trend clearly indicates that the backward reaction is favored over the forward reaction for the NO_2 formation mechanism. Initiation by intramolecular H transfer has the lowest activation energy among the three paths. However, its heat of reaction indicates that the reverse reaction has significantly lower barrier (18.48 kcal/mol) than forward reaction making the reverse reaction more probable. These energy

scans clearly indicate that intermolecular H transfer is the most likely initiation pathway that can form a stable chemical intermediate. This trend agrees well with the observed initiation reaction statistics shown in Figure 6.

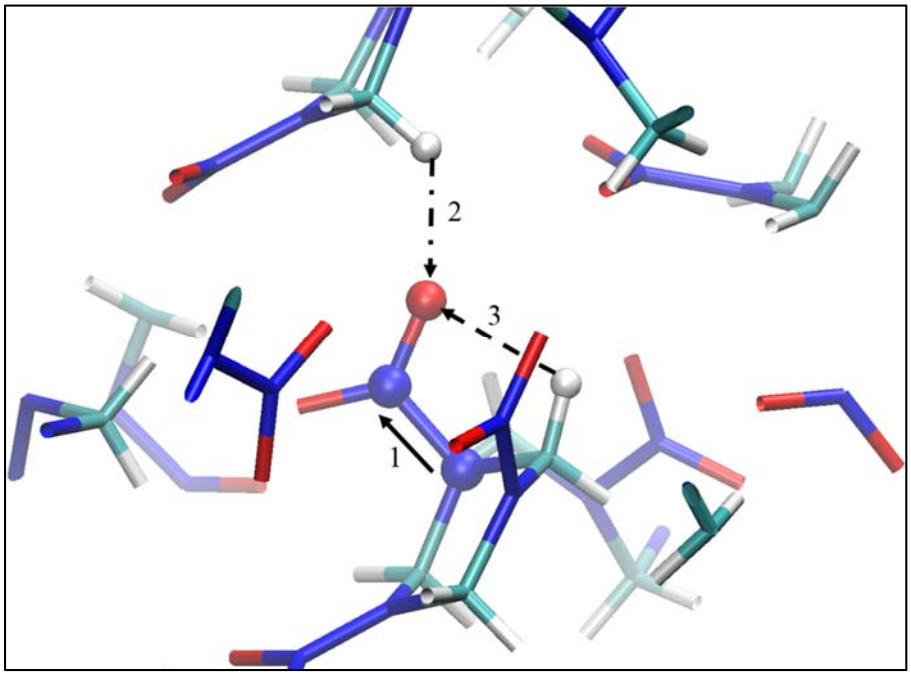

Figure 7: Close-up view of the unit cell used in energy scans, 1: N-N bond cleavage, 2: intermolecular H transfer, 3: Intramolecular H transfer, Nitrogen- Blue, Oxygen- Red, Carbon- Green, Hydrogen- White

Table 1: Estimated activation energies and heat of reactions of initiation of RDX from ReaxFF inside the γ-phase crystal

Initiation Pathway	Activation Energy (kcal/mol)	Heat of Reaction (kcal/mol)
N-N Bond Cleavage	71.85	62.40
Intermolecular H Transfer	68.28	15.28
Intramolecular H Transfer	56.30	37.82

Once these initial pool of smaller radicals is formed, then these radicals react further with the neighboring RDX molecules forming the short lived polyradical complexes as seen in the mass fraction analysis. As mentioned previously, these heavy polyradical complexes constantly

exchange the constituents species with the surrounding molecules due to very high density and hence the actual chemical composition of such complexes is constantly changing.Tracking the exact chemistry that leads to the thermal runaway region is a challenging task due to small lifetime of species and high reactivity. So, we have to depend more on the stable gas-phase products with higher lifetime. Chemical insight about the decomposition chemistry from the molecular population of dominant chemical species is often fraught with perils of over-simplification but we observe an interesting correlation of the chemical events that needs further investigation.

Evolution of intermediate radicals

Figure 8 shows the population of the dominant intermediate chemical species as a function of time. These radicals can be broadly divided into two groups: H-acceptors and H-donors which participate in H-transfer reactions. The acceptor species ($C_3H_7O_6N_6$) are more likely to eliminate the OH thereby forming l-nitroso-3, 5-dinitrohexahydro-s-triazine (ONDNTA). Figure 8 shows the significant accumulation of the ONDNTA until 80ps. The ONDNTA has been found experimentally in gas phase and it was found that these products condense on the surface of RDX particles and in the regions between the RDX particles[11]. However, the observed chemical mechanism in our simulations that leads to formation of these radicals differ from what was mentioned in the literature[9]. In the literature, it was mentioned that ONDNTA was formed by the cleavage of N-N bond of RDX molecules which was followed by the recombination with NO from another reaction. However, our simulations show negligible NO until 80 ps (Figure 9a). Instead, we observe OH and $C_3H_6O_5N_6$ (Figure 8) radicals during the ignition delay phase. These trends indicate that in the reactive MD simulations, most of the ONDNTA radicals are formed by the OH elimination (Table 2).

To explain this observed trend of ONDNTA formation, we again performed energy scans on the two possible pathways that H-acceptor species can undergo. We used the product state of intermolecular H-transfer initiation pathway ($C_3H_7O_6N_6$) as the starting state for these energy scans. Similar to the initiation energy scans, these calculations were done on the periodic unit cell of γ-RDX. The estimated activation energies and the heats of reaction of the OH and the HONO elimination pathways are shown in Table 2. The energy scans show that the OH elimination has considerably lower activation energy and heat of formation than the HONO elimination. This preference for the OH elimination results in a significant accumulation of ONDNTA during the ignition delay phase. Additional comparison between ReaxFF and DFT activation enthalpies for

the hydrogen and oxygen transfer reactions that intermediate radicals can undergo in gas phase is provided in supplementary information. We used the gas phase reactions for those additional calculations because we could not find any DFT data in the literature for such reactions in condensed phase.

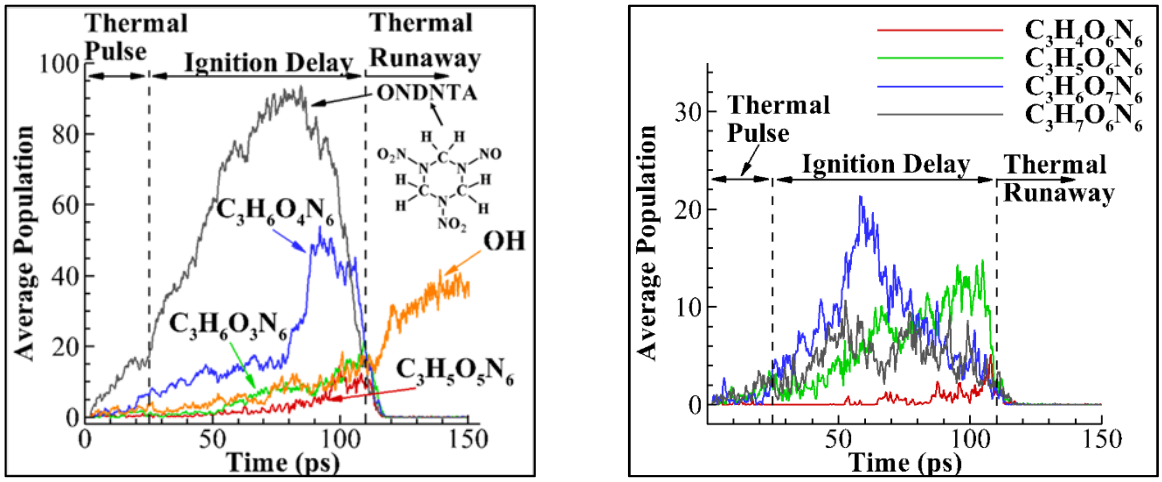

H-acceptor radicals H-donors radicals

Figure 8: Evolution of reaction intermediates with triazine ring including accumulation of experimentally known intermediate ONDNTA shown.

Table 2: Estimated activation energies and heats for reactions of intermediate chemical steps

Reaction	Activation Energy (kcal/mol)	Heat of reaction (kcal/mol)
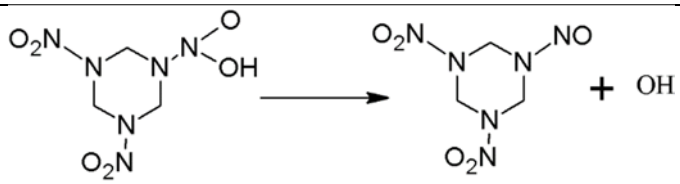 ONDNTA	31.11	9.24
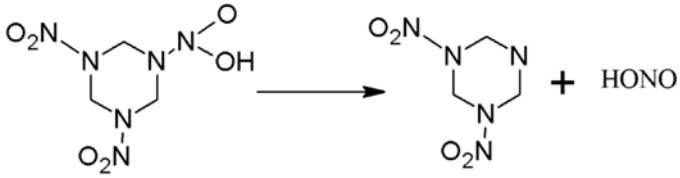	56.11	43.59

It should be noted that although the actual number of OH radicals during the ignition delay phase is small, it is mainly because the OH is extremely reactive and hence combines readily with other fragments. We see significant accumulation of the OH radicals only in the thermal runaway stage due to the extremely fast production rate of the OH radicals compared to the consumption rate. Apart from the hydrogen acceptor species, we also observed $C_3H_5O_6N_6$ radicals which are originally formed when a RDX molecule donates a hydrogen to its neighbor. These species are continually present during the ignition delay phase indicating a constant production through the hydrogen transfer reactions (Figure 8). Our trajectory analysis indicates that the CH group of these hydrogen donor radicals is more likely to combine with the OH (forming C-OH bond) to form $C_3H_6O_7N_6$ radical (Figure 8). These observed trends further corroborate the initial conclusion that the hydrogen transfer chemistry dominates the ignition delay phase.

Formation of stable gas products

The remaining important question on the chemistry of RDX ignition is the creation of stable gas-products. Previous studies on the decomposition of the ONDNTA found that it decomposes first into N_2, NO_2 and non-volatile residue (NVR)[11]. NVR further breaks down into CH_2O, N_2O and CO. However, our simulations do not show noticable amounts of N_2O, CO and CH_2O in the ignition delay and thermal runaway phases. Instead, we observe a sharp drop in the ONDNTA population with simultaneous increase in concentration of $C_3H_6O_4N_6$ and $C_3H_6O_3N_6$ radicals (Figure 8a). Thus, ONDNTA continues to loose peripheral oxygen atoms and participate in the formation of heavier polyradicals. Once the ignition to thermal runaway transition (beyond 110ps) occurs, we observe the sudden rise in final stable products accompanied by the ring opening reactions. Figure 9b shows that N_2 is the most dominant final product in this rapid thermal runaway stage. Our trajectory analysis shows that more than 95% of the N_2 population is made of the constituent nitrogen atoms that were part of the same RDX molecule. This trend clearly shows that more than 66% of N-N bonds are not cleaved before the ring opening reactions. The remaining 33% of N-N bonds are broken either by NO elimination or by HONO elimination (Figure 9a). This N-N cleavage leaves behind NC group that further forms NCOH radical as can be seen in Figure 9b. These NCOH radical species are formed either by OH combining with RDX ring at CH group (as explained earlier) before the ring opening or by NC radical combining with OH radical after the ring opening. N_2 is followed by water as the 2nd most dominant reaction product. This is mainly produced by the OH radicals reacting with the hydrogen of CH_2 groups of RDX rings.

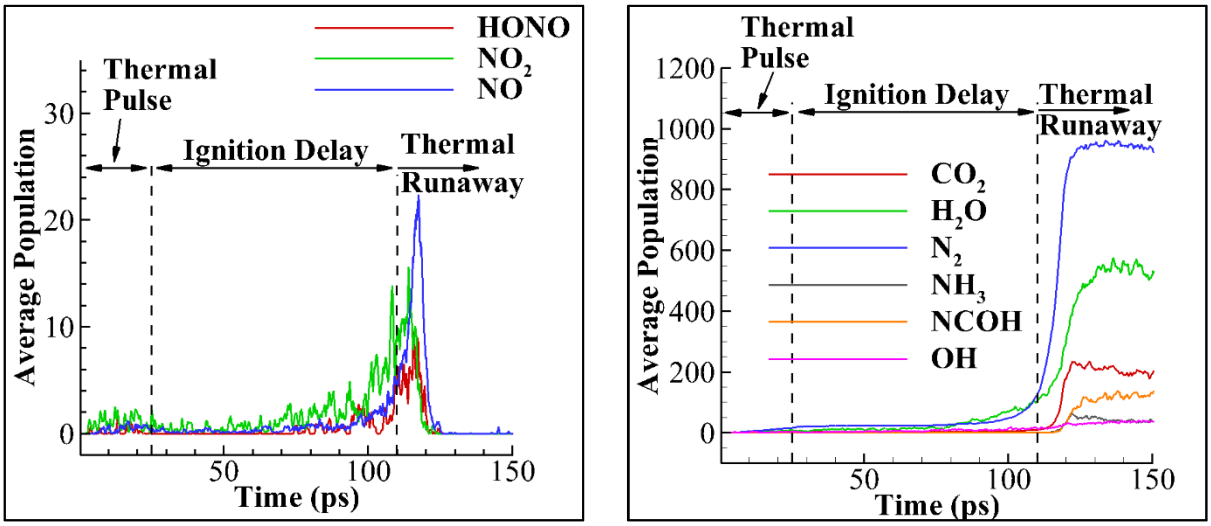

(a) (b)

Figure 9: Evolution final products during ignition to thermal runaway transition

The results are a snapshot of many important issues which need to be addressed in the future. The chemistry of the exothermic steps during the runaway stage is still highly complex and we reverted to the gas-phase products based analysis. Identification of the reactant molecules which connects the products in the reaction network will require better algorithms as many parts of the same molecule can be reacting within a very short period of time. This creates a challenge for the traditional chemical analysis of enthalpy and rates. The 2000 K used in the study is not the exact critical temperature for RDX ignition from a nanoscale hot spot. The preliminary results presented here indicate that for a overdriven thermal ignition from a hot spot, the chemistry in the RMD simulations has matured enough to show the expected set of events in a high-density reactive environment. Some key reactive events are validated using the DFT calculations which show a reasonable agreement in activation energy.

Conclusion

In summary, we have demonstrated the RMD-based chemical model which shows some unique sequence of the reactive events leads to the formation of a thermal deflagration front in condensed-phase γ-RDX crystal when 5% of the solid is subjected to a thermal stimuli to mimic a thermal hot spot. We have performed the simulations with an improved version of ReaxFF parameters which has combined the nitramine training set with the C/H/O combustion training set. We have used an extremely conservative setting of 0.01 fs time step in our calculation to ensure

the uniqueness of the chemistry. This is beneficial due to the high degree of H transfer and ultrafast reaction chemistry in the deflagration stage. Among the key observations, analysis of the trajectories show that the traditional initiation mechanism involving NO_2 formation by the homolytic cleavage of N-N bond is not favored in condensed phase γ-RDX. Instead, the initiation chemistry is dominated by the intermolecular and intramolecular hydrogen transfer reactions. The subsequent radicals then combine with each other forming short-lived heavier polyradical complexes with triazine rings intact and continues to lose the peripheral hydrogen and oxygen atoms during the ignition delay phase. The reactive mixture eventually reaches a temperature and a chemical composition which transitions to the thermal runaway regime where the opening of the C-N rings and creation of stable gas products are observed. It is difficult to pinpoint if the ring opening leads to a sudden rise in temperature and pressure or creation of stable gas products fuel further ring openings. The entire simulation domain reacts spontaneously towards the decomposition products until it runs out of fuel in the reaction domain. The simulations identify a key radical, ONDNTA, which dominates how the rest of the polyradicals and the stable gas products are formed. The chemistry described in this work is applicable to the P-V-T states created by the hot spot with transient effects controlled by the duration of the external thermal stimuli. The model chemistry presented in this work has important applicability for the condensed phase thermal decomposition of a broad range of propellants and CHNO-based energetic materials. The simulation cell size and aspect ratios will change the kinetics purely due to the thermal conductivity and the possible difference in hot spot growth kinetics along different directions. Ongoing calculations using different sized unit cells and aspect ratios to uncover the universal scaling relationships between the hot spot size, critical temperature and growth kinetics are being performed. The complexity of the chemistry will continue to be an impediment for a full validation of the individual steps in the trajectory with nearly 150,000 reactive events. For validation of the chemistry, we extracted the potential energy surface from ReaxFF for some key initiation steps in the γ-RDX lattice and compared them with DFT and higher-level (MP2) theory calculated values using QM/MM methods. The polyradicals are too large and dynamic in size for a realistic investigation using DFT. The ability to separate critical intermediates in high-pressure/high-temperature conditions afforded by the reactive molecular dynamics can be complemented by further calculations on understanding the stability of the polyradical species, their formation from the ONDNTA and the causes for attaining the criticality.

Corresponding Author
*Email: santc@illinois.edu

Notes
The authors declare no competing financial interests.

Acknowledgement

The authors acknowledge stimulating discussion with Professors Thomas Sewell, Scott Stewart and Dana Dlott on the reactive simulations. We also thank Professor Yogi Gupta and Zbigniew Dreger in Washington State University for their insights on RDX decomposition experiments and spectroscopic measurements. We acknowledge funding from DTRA grant# HDTRA1-13-1-0018.

References

1. Zel'dovich, Y. B., On the Theory of the Propagation of Detonation in Gaseous Systems. *Soviet Journal of Experimental and Theoritical Physics* **1940**, *10*, 542.
2. Melius, C., Thermochemical Modeling: Ii. Application to Ignition and Combustion of Energetic Materials. In *Chemistry and Physics of Energetic Materials*, Bulusu, S., Ed. Springer Netherlands: 1990; Vol. 309, pp 51-78.
3. Sewell, T. D.; Thompson, D. L., Classical Dynamics Study of Unimolecular Dissociation of Hexahydro-1,3,5-Trinitro-1,3,5-Triazine (Rdx). *The Journal of Physical Chemistry* **1991**, *95*, 6228-6242.
4. Zhao, X.; Hintsa, E. J.; Lee, Y. T., Infrared Multiphoton Dissociation of Rdx in a Molecular Beam. *The Journal of Chemical Physics* **1988**, *88*, 801-810.
5. Behrens, R.; Bulusu, S., Thermal Decomposition of Energetic Materials. 3. Temporal Behaviors of the Rates of Formation of the Gaseous Pyrolysis Products from Condensed-Phase Decomposition of 1,3,5-Trinitrohexahydro-S-Triazine (Rdx). *The Journal of Physical Chemistry* **1992**, *96*, 8877-8891.
6. Chakraborty, D.; Muller, R. P.; Dasgupta, S.; Goddard, W. A., The Mechanism for Unimolecular Decomposition of Rdx (1,3,5-Trinitro-1,3,5-Triazine), an Ab Initio Study. *The Journal of Physical Chemistry A* **2000**, *104*, 2261-2272.
7. Yetter, R. A.; Dryer, F. L.; Allen, M. T.; Gatto, J. L., Development of Gas-Phase Reaction Mechanisms for Nitramine Combustion. *Journal of Propulsion and Power* **1995**, *11*, 683-697.
8. Chakraborty, D.; Muller, R.; Dasgupta, S.; Goddard, W., III, A Detailed Model for the Decomposition of Nitramines: Rdx and Hmx. *Journal of Computer-Aided Materials Design* **2001**, *8*, 203-212.
9. Kuo, K. K.; Acharya, R., Thermal Decomposition and Combustion of Nitramines. In *Applications of Turbulent and Multiphase Combustion*, John Wiley & Sons, Inc.: 2012; pp 72-142.
10. Brill, T. B.; Brush, P. J.; Patil, D. G.; Chen, J. K., Chemical Pathways at a Burning Surface. *Symposium (International) on Combustion* **1992**, *24*, 1907-1914.
11. Maharrey, S.; Behrens, R., Thermal Decomposition of Energetic Materials. 5. Reaction Processes of 1,3,5-Trinitrohexahydro-S-Triazine Below Its Melting Point. *The Journal of Physical Chemistry A* **2005**, *109*, 11236-11249.

12. Wang, J.; Brower, K. R.; Naud, D. L., Evidence of an Elimination Mechanism in Thermal Decomposition of Hexahydro-1,3,5-Trinitro-1,3,5-Triazine and Related Compounds under High Pressure in Solution. *The Journal of Organic Chemistry* **1997**, *62*, 9055-9060.
13. Schweigert, I. V., Quantum Mechanical Simulations of Condensed-Phase Decomposition Dynamics in Molten Rdx. *Journal of Physics: Conference Series* **2014**, *500*, 052039.
14. Brennan, J. K.; Lísal, M.; Moore, J. D.; Izvekov, S.; Schweigert, I. V.; Larentzos, J. P., Coarse-Grain Model Simulations of Nonequilibrium Dynamics in Heterogeneous Materials. *The Journal of Physical Chemistry Letters* **2014**, *5*, 2144-2149.
15. van Duin, A. C. T.; Dasgupta, S.; Lorant, F.; Goddard, W. A., Reaxff: A Reactive Force Field for Hydrocarbons. *The Journal of Physical Chemistry A* **2001**, *105*, 9396-9409.
16. Chenoweth, K.; van Duin, A. C. T.; Goddard, W. A., Reaxff Reactive Force Field for Molecular Dynamics Simulations of Hydrocarbon Oxidation. *The Journal of Physical Chemistry A* **2008**, *112*, 1040-1053.
17. Strachan, A.; Kober, E. M.; van Duin, A. C.; Oxgaard, J.; Goddard, W. A., Thermal Decomposition of Rdx from Reactive Molecular Dynamics. *The Jurnal of Chemical Physics* **2005**, *122*, 54502.
18. Han, S.-p.; van Duin, A. C. T.; Goddard, W. A.; Strachan, A., Thermal Decomposition of Condensed-Phase Nitromethane from Molecular Dynamics from Reaxff Reactive Dynamics. *The Journal of Physical Chemistry B* **2011**, *115*, 6534-6540.
19. Shan, T.-R.; van Duin, A. C. T.; Thompson, A. P., Development of a Reaxff Reactive Force Field for Ammonium Nitrate and Application to Shock Compression and Thermal Decomposition. *The Journal of Physical Chemistry A* **2014**, *118*, 1469-1478.
20. Zhou, T.; Song, H.; Liu, Y.; Huang, F., Shock Initiated Thermal and Chemical Responses of Hmx Crystal from Reaxff Molecular Dynamics Simulation. *Physical Chemistry Chemical Physics* **2014**, *16*, 13914-13931.
21. Wood, M. A.; van Duin, A. C. T.; Strachan, A., Coupled Thermal and Electromagnetic Induced Decomposition in the Molecular Explosive Ahmx; a Reactive Molecular Dynamics Study. *The Journal of Physical Chemistry A* **2014**, *118*, 885-895.
22. Furman, D.; Kosloff, R.; Dubnikova, F.; Zybin, S. V.; Goddard, W. A.; Rom, N.; Hirshberg, B.; Zeiri, Y., Decomposition of Condensed Phase Energetic Materials: Interplay between Uni- and Bimolecular Mechanisms. *Journal of the American Chemical Society* **2014**, *136*, 4192-4200.
23. Sergeev, O. V.; Yanilkin, A. V., Molecular Dynamics Simulation of Combustion Front Propagation in a Petn Single Crystal. *Combust Explos Shock Waves* **2014**, *50*, 323-332.
24. An, Q.; Goddard, W. A.; Zybin, S. V.; Jaramillo-Botero, A.; Zhou, T., Highly Shocked Polymer Bonded Explosives at a Nonplanar Interface: Hot-Spot Formation Leading to Detonation. *The Journal of Physical Chemistry C* **2013**, *117*, 26551-26561.
25. An, Q.; Zybin, S. V.; Goddard, W. A.; Jaramillo-Botero, A.; Blanco, M.; Luo, S.-N., Elucidation of the Dynamics for Hot-Spot Initiation at Nonuniform Interfaces of Highly Shocked Materials. *Physical Review B* **2011**, *84*, 220101.
26. Nomura, K.-i.; Kalia, R. K.; Nakano, A.; Vashishta, P., Reactive Nanojets: Nanostructure-Enhanced Chemical Reactions in a Defected Energetic Crystal. *Applied Physics Letters* **2007**, *91*, 183109.
27. Manaa, M. R.; Fried, L. E., The Reactivity of Energetic Materials under High Pressure and Temperature. *Adv Quantum Chem* **2014**, *69*, 221-252.
28. Manaa, M. R.; Fried, L. E.; Melius, C. F.; Elstner, M.; Frauenheim, T., Decomposition of Hmx at Extreme Conditions: A Molecular Dynamics Simulation. *J Phys Chem A* **2002**, *106*, 9024-9029.
29. Manaa, M. R.; Reed, E. J.; Fried, L. E.; Goldman, N., Nitrogen-Rich Heterocycles as Reactivity Retardants in Shocked Insensitive Explosives. *Journal of the American Chemical Society* **2009**, *131*, 5483-5487.
30. Joshi, K. L.; Raman, S.; van Duin, A. C. T., Connectivity-Based Parallel Replica Dynamics for Chemically Reactive Systems: From Femtoseconds to Microseconds. *The Journal of Physical Chemistry Letters* **2013**, *4*, 3792-3797.

31. Zou, C.; Raman, S.; van Duin, A. C. T., Large-Scale Reactive Molecular Dynamics Simulation and Kinetic Modeling of High-Temperature Pyrolysis of the Gloeocapsomorphaprisca Microfossils. *The Journal of Physical Chemistry B* **2014**, *118*, 6302-6315.
32. Tarver, C. M.; Chidester, S. K.; Nichols, A. L., Critical Conditions for Impact- and Shock-Induced Hot Spots in Solid Explosives. *J Phys Chem-Us* **1996**, *100*, 5794-5799.
33. Dreger, Z. A.; Gupta, Y. M., Phase Diagram of Hexahydro-1,3,5-Trinitro-1,3,5-Triazine Crystals at High Pressures and Temperatures. *The Journal of Physical Chemistry A* **2010**, *114*, 8099-8105.
34. Clark, S. J.; Segall, M. D.; Pickard, C. J.; Hasnip, P. J.; Probert, M. J.; Refson, K.; Payne, M. C., First Principles Methods Using Castep. *Z Kristallogr* **2005**, *220*, 567-570.
35. Aktulga, H. M.; Fogarty, J. C.; Pandit, S. A.; Grama, A. Y., Parallel Reactive Molecular Dynamics: Numerical Methods and Algorithmic Techniques. *Parallel Computing* **2012**, *38*, 245-259.
36. Plimpton, S., Fast Parallel Algorithms for Short-Range Molecular Dynamics. *Journal of Computational Physics* **1995**, *117*, 1-19.
37. Liu, L.; Liu, Y.; Zybin, S. V.; Sun, H.; Goddard, W. A., Reaxff-Lg: Correction of the Reaxff Reactive Force Field for London Dispersion, with Applications to the Equations of State for Energetic Materials. *The Journal of Physical Chemistry A* **2011**, *115*, 11016-11022.